

Deep Learning Classification of The Ground Penetrating Radar Data to Determine Underground Cavities Under the Road

Rohit Shrestha*, Zhang Zhihou, Sulaiman Khan, Xiaoyan Zhao

Faculty of Geosciences and Environmental Engineering, Southwest Jiaotong University, Chengdu, Sichuan 611756, China

Abstract. This study examines the effectiveness of ground penetrating radar (GPR) in detecting and categorizing diseases hidden beneath urban road surfaces. Convolutional neural networks (CNNs), specifically transfer learning using AlexNet, enhance classification accuracy of cavity shapes to 90.5%. Even with limited data, this strategy performs better than current ones. An examination of subsurface cavity data from 1965 reveals four main types: water-rich bodies, hollow bodies, empty bodies, and loose bodies. These classifications are critical for assessing road hazards including sinkholes and voids. The precise interpretation of image features associated with cavity disorders remains challenging. This is due to several factors, including geological, human, and environmental impacts. Accurately assessing and identifying picture elements associated with dental issues remains challenging. Many additional variables can also contribute to subterranean diseases and cavities, including as environmental and geological causes, the physical and chemical characteristics of geotechnical materials, engineering activities carried out by humans, and the impact on the population or economics of the subterranean community.

Keywords: Diseases; CNN; Cavities; AlexNet.

Email: rohishrestha@my.swjtu.edu.cn, logicprimer@163.com,

1. Introduction

One significant geophysical technique regarded as nondestructive is using ground-penetrating radar (Al-Qadi & Lahouar, 2005; Daniels, 2004). Ground penetrating radar (GPR) uses propagating electromagnetic (EM) waves to detect changes in the electromagnetic properties of the shallow subsurface. The primary factor influencing the creation of reflections (or the contrast between layers) is the relative permittivity contrast between the target and the background material, which controls the propagation velocity of electromagnetic waves (Al-Qadi & Lahouar, 2005; Baker et al., 2007).

The ability of a substance to retain electromagnetic energy before allowing that energy to pass through is known as its relative permittivity, and it may be measured

in a laboratory (Baker et al., 2007; Kuliczowska, 2016). The process of creating high-performance antennas is uniform and might be seen as a generalized optimization issue, even though the specifications for their kind and design differ based on the GPR configuration. In this instance, the framework for developing and enhancing GPR antennas (Liu et al., 2018; Zhang et al., 2023; Zhao et al., 2015).

To train the network model, actual radar data is used. Water anomalies and subgrade settlement are two distinct disorders for which more photos are first collected using the CycleGAN neural network. This helps to address the problem of inadequate training outcomes caused by insufficient data. Subsequently, the network is trained semi-supervised using both labeled raw data and expanded unlabeled data. This addresses low recognition

accuracy in the GPR domain caused by difficult access to annotated radar data. (Yang et al., 2024).

In this article, we conduct an extensive analysis of the feasibility of categorizing different types of cavities in ground penetrating radar (GPR) data through the application of convolutional neural network (CNN) techniques, particularly AlexNet.

It performed an extensive assessment of our approaches by measuring concrete layers in the field and comparing the findings with GPR software in different urban situations. All in all, this research has the potential to greatly advance our knowledge of subterranean spaces and provide insightful new information for future subterranean building projects.

2. Materials and Methods

Stream-X, an Italian three-dimensional ground-penetrating radar, and ProEx, a Swedish multi-angle geological radar, are two of the portable two-dimensional geological radars used in this investigation, along with GPS and other various equipment.

The antenna that transmits electromagnetic waves into a subsurface medium is followed by an antenna that receives the reflected signals and uses the difference in dielectric constants to calculate the reflectance and signal strength.

GPR investigations focus on under-road concerns because the dielectric properties of air-filled and water-filled locations differ. On a PC with an Intel Core i5-12400F and an NVIDIA GeForce RTX 3060, GprMax was used to mimic road modules.

A commercial 3D GPR gadget was utilized to record field data while an automobile was in motion. Classification

analysis was performed in MATLAB using CNN and the AlexNet approach.

2.1. Convolutional Neural Network (CNN)

In this work, a CNN is used to categorize subsurface cavities, as shown in Fig. 1. 600 epochs of training with a linear learning rate of 0.0001 and a validation frequency of 50 are conducted on AlexNet using the sgdm.

The effectiveness of the model is assessed using an alternative test set. Pooling layers minimize the number of features while convolutional layers identify certain areas of the picture. ReLU activation, five convolutional layers, and 96 filters (11x11) make up the CNN's input layer.

The following layers have filter numbers of 128, 384, 192, and 128, with kernel sizes of 5x5, 3x3, 3x3, and 3x3. Using 3x3 convolution and pooling operations with a stride of 1x1, three 2D grouped convolutional layers are employed. The output layer's four distinct cavity types get Softmax activation.

The settings are varied throughout 600 epochs of AlexNet optimization using a cross-entropy loss function and a starting rate of 0.0001. MATLAB uses transfer AlexNet or a customized version to mimic GPR data processing. Equations (1-3) define recall, precision, and F score indices that are used to evaluate performance.

$$Precision = \frac{true\ positive}{true\ positive + false\ positive} \times 100\% \quad (1)$$

$$Recall = \frac{true\ positive}{true\ positive + false\ negative} \times 100\% \quad (2)$$

$$F - score = \frac{2 \times Precision \times Recall}{Precision + Recall} \quad (3)$$

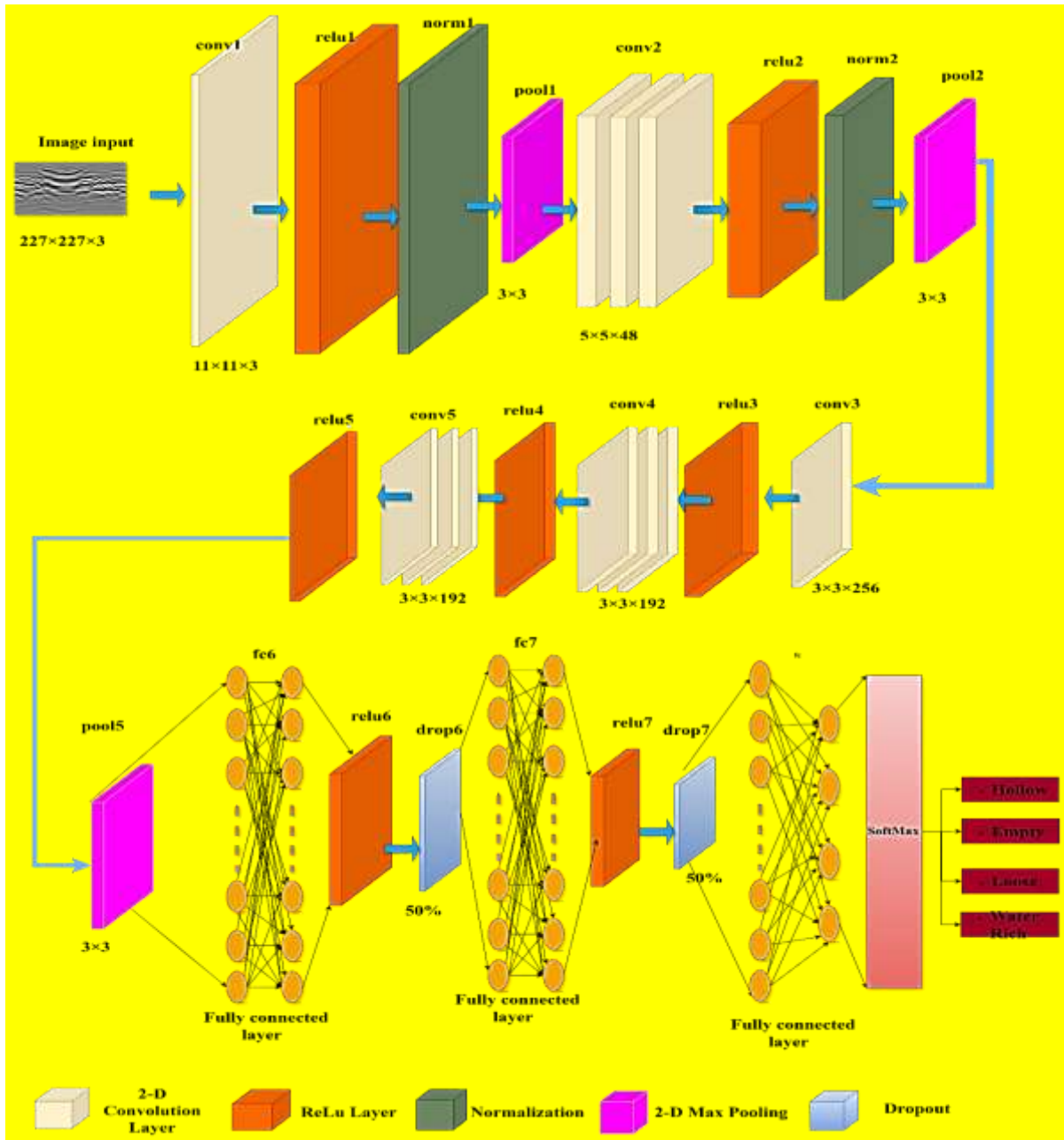


Fig. 1. Architecture of CNN AlexNet

3. Results and Discussion

3.1. Classification of Cavities and Analysis

The characterization and classification of road cavities and subterranean diseases rely on various forward model simulations. A simulation model of the radar profile picture and the shape of the cavities are used to classify common underground illnesses into hollow, empty body, loose body, and water-rich body categories. A number of external interface factors classify the cavities under the surface of the road, such as the degree of coupling between the antenna and the road, pipeline interfaces (metal, nonmetal, pipe culvert, and manhole cover),

electromagnetic interfaces, and ground interfaces (ground gravel, ground overhead wires, and ground metal objects) (Jin-sung et al., 2020; Lee et al., 2022).

The results of the categorization indicate noteworthy patterns in extensive research with 1965 cavities. A sizable portion of the cavity samples - 778 samples, or 39.59%—were identified as hollow bodies. It is likely that cavities in this group have a distinct and enclosed interior, which contributes to the reason for their name, hollow. Furthermore, a sizable fraction - 584 samples, or 29.72 percent - are categorized as empty bodies. This

word refers to cavities that have comparatively little material inside of them, suggesting that either very little or no material is there at all. Additionally, 590 samples (30.03%) were found to be loose corpses throughout the investigation, suggesting that there may have been some internal disorder or mobility within these cavities. This class may describe cavities whose internal components

are less constrained or more fluid-like. It's interesting to note that 13 samples - or 0.66% of the total - fit the description of bodies rich in water. This arrangement highlights the variety of compositions observed in the samples under examination and highlights the substantial amount of water contained in the voids.

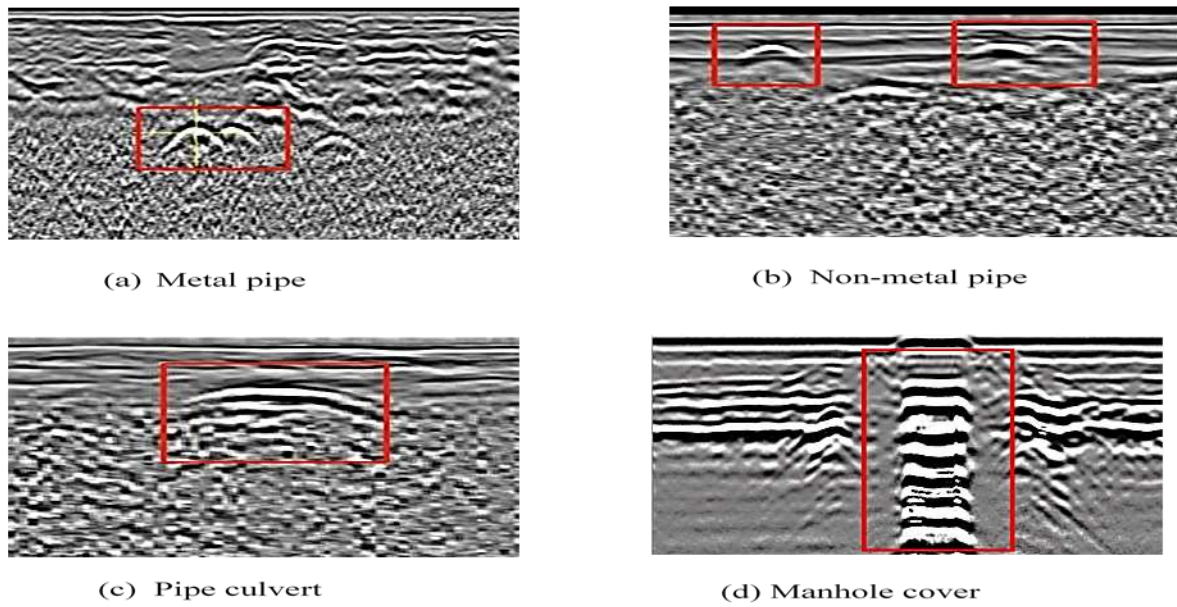


Fig. 2. Underground interference

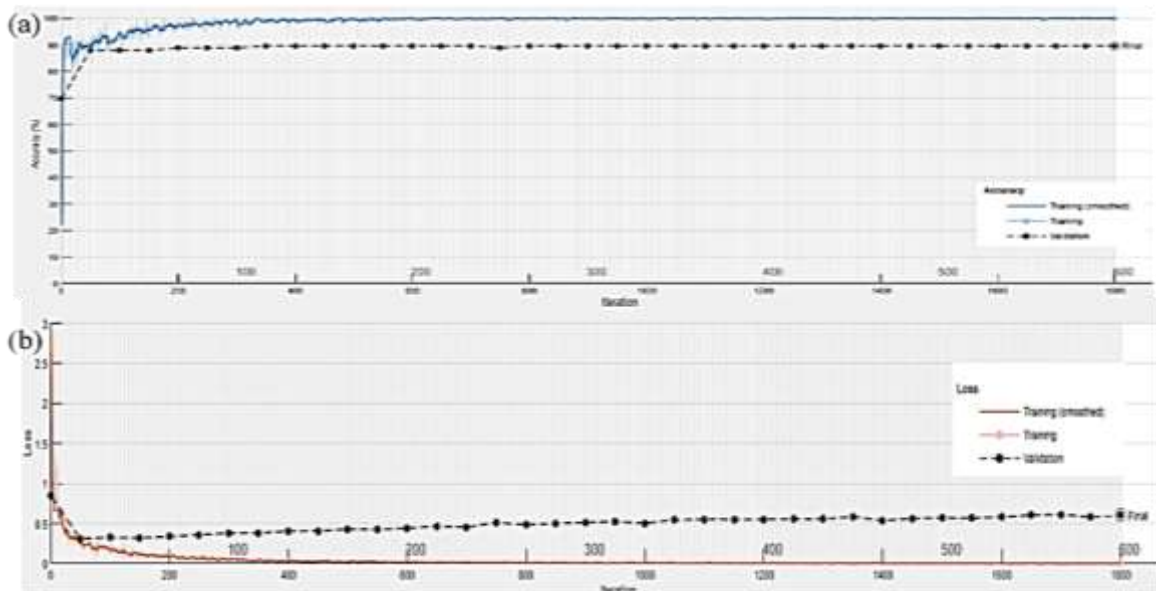


Fig. 3 Testing accuracy and training loss validation of the transfer AlexNet



Fig. 4. Confusion matrix

A significant advance in the discipline is the ability of the AlexNet architecture to analyze deep features allows for the classification of the geometry of subsurface cavities through transfer learning. AlexNet's effectiveness in classifying different types of underground cavities is clear, with a maximum number of iterations of 1800 and 600, a learning rate of 0.0001, and the ability to attain 90.5% accuracy in training data validation in very short amounts of time—7 minutes and 58 seconds. The confusion matrix's visual representation in Figures. 3 and 4 offers a thorough summary of the classification results and highlights the model's remarkable recall rates and precision in distinguishing between various cavity morphological types.

For the real-time subsurface cavity type classification before GPR scans, deep CNN models connected to GPR equipment also show a lot of potential. The precision ratings of 90% and 100% for loose and empty bodies, and hollow body cavities, respectively, show how effective this method is. It is evident that there are issues related to the lack of data for bodies rich in water because this category received 0 recall and precision ratings. While the model's 100% recall for hollow body cavities is impressive, its 14.3% and 25% recall for loose and empty

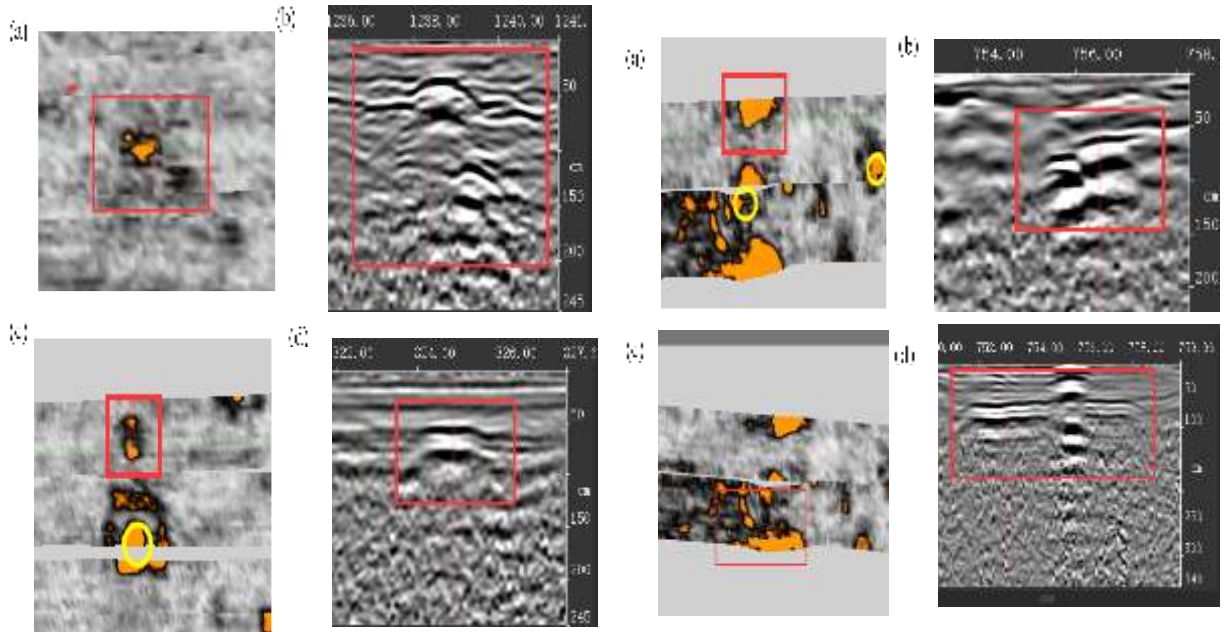
bodies, respectively, might be improved. As Table 1 shows, the computed F scores offer a thorough assessment of the model's performance and point out areas that require development. The model's performance is particularly bad in classifying empty and loose bodies properly, as indicated by F values of 25.02 and 40, respectively.

The profiles of hollow, inflated spherical and cubic voids show unique features in ground-penetrating radar (GPR) imaging. In B-scan radar profiles, spherical voids exhibit downward hyperbolic apertures, but cubic voids display forward continuous flat plates with numerous waves and diffraction visible. These holes generate a complex electromagnetic response with an overall amplitude of less than 0.2 m and a reflection clearance. The incident and top reflected waves are phase- and frequency-aligned, with the bottom reflected wave exhibiting a white-black-white color pattern and traveling at a higher frequency than the background field. The GPR B-scan profiles of loose bodies show many internal waves with isotropic reflection at the top and less pronounced diffraction, which together result in an irregular internal waveform with a black-white-black color pattern. Radar waves attenuate dramatically in water-rich environments,

resulting in intense surface reflections and quick attenuation. The spectrum exhibits multiple reflections and phase inversions, as seen in Figure 5, where the bottom reflected wave aligns with the incident wave while the top reflected wave opposes it. A high brightness white-black pattern is repeated by the bottom reflected wave, which has a frequency lower than the background field.

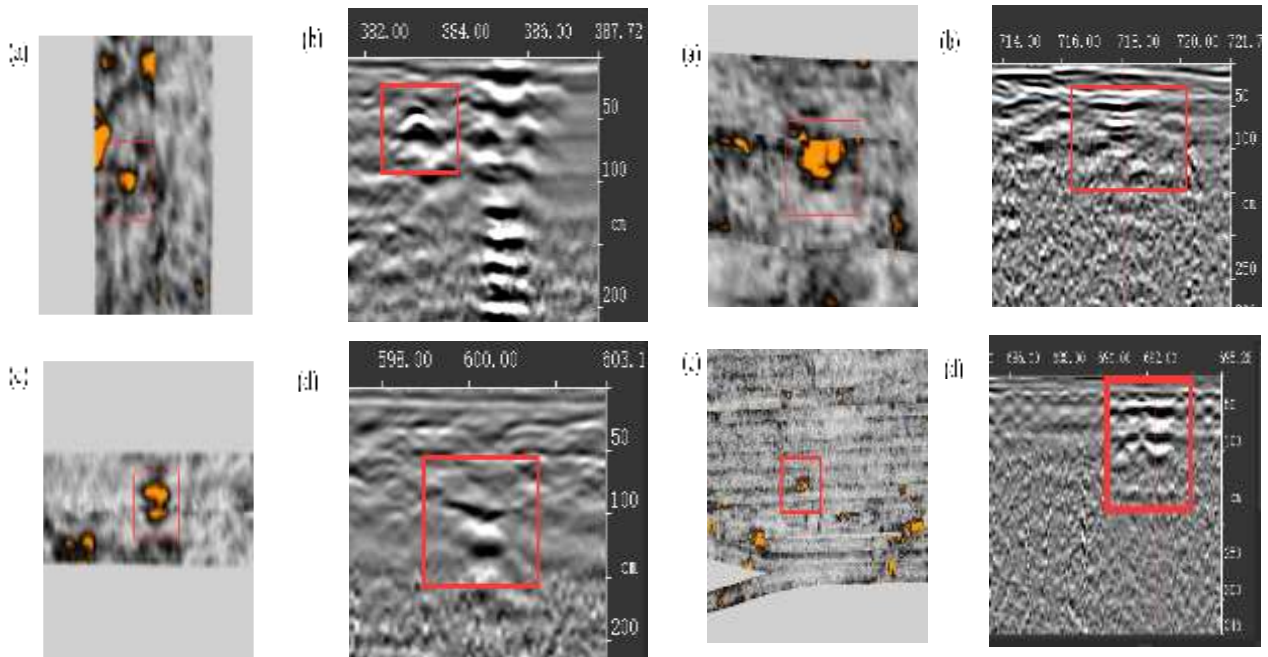
Table 1 Analytical outcomes of the parameters acquired using AlexNet

Parameters	Precision	Recall	F Score
Hollow	90.40	100.00	94.96
Empty	100.00	14.31	25.02
Loose	100.00	25.00	40.00



1. The hollow body cavities

2. The empty body cavities



3. The loose body cavities

4. The water-rich body cavities

Fig. 5 GPR profile images for cavities observed under the road (a) & (c) C-scan (b) & (d) B-scan profile

4. Conclusions

In underground environments and on road infrastructure, the study's results underscore the significance of employing forward simulation models of ground-penetrating radar (GPR) image profiles for void classification and localization. AlexNet's effectiveness in classifying different types of underground cavities is clear, with a maximum number of iterations of 1800 and 600, a learning rate of 0.0001, and the ability to attain 90.5% accuracy in training data validation in very short amounts of time - 7 minutes and 58 seconds. The precision ratings of 90% and 100% for loose and empty bodies, and hollow body cavities, respectively, demonstrate the effectiveness of this method. However, there are issues due to the lack of data for bodies with high water content, as this category received 0 recall and precision ratings. Although the model's 100% recall for hollow body cavities is impressive, its recall rates of 14.3% and 25% for loose and empty bodies, respectively, could be improved. Although the AlexNet-based classification faced challenges in identifying water-rich entities due to insufficient data, it proved effective in identifying hollow and empty spaces. While improvements are needed, particularly in detecting empty and loose bodies, it seems that the proposed CNN model could reliably detect various types of subsurface cavities using GPR B-scans. Therefore, enhancing the model's capabilities could improve its ability to categorize underground caverns.

References

Al-Qadi, I. L., & Lahouar, S. (2005). Measuring layer thicknesses with GPR—Theory to practice. *Construction and building materials*, 19(10), 763-772.

Baker, G. S., Jordan, T. E., & Pardy, J. (2007). An introduction to ground penetrating radar (GPR).

Daniels, D. J. (2004). *Ground penetrating radar* (Vol. 1). Iet.

Jin-sung, Y., Minkyoo, Y., Sehwan, P., & Junkyeong, K. (2020). Technique for Detecting Subsurface Cavities of Urban Road Using Multichannel Ground-penetrating Radar Equipment. *Sensors & Materials*, 32.

Kuliczowska, E. (2016). An analysis of road pavement collapses and traffic safety hazards resulting from leaky sewers. *The Baltic Journal of Road and Bridge Engineering*, 11(4), 251-258.

Lee, S., Park, J.-J., & Cho, B. H. (2022). Management of cavities under flexible pavement road network in metropolitan area: Detection, evaluation, and rehabilitation. *Developments in the Built Environment*, 12, 100091.

Liu, H., Long, Z., Han, F., Fang, G., & Liu, Q. H. (2018). Frequency-domain reverse-time migration of ground penetrating radar based on layered medium green's functions. *IEEE Journal of Selected Topics in Applied Earth Observations and Remote Sensing*, 11(8), 2957-2965.

Yang, Y., Huang, L., Zhang, Z., Zhang, J., & Zhao, G. (2024). CycleGAN-Based Data Augmentation for Subgrade Disease Detection in GPR Images with YOLOv5. *Electronics*, 13(5), 830.

Zhang, W., Xin, G., Long, G., & Song, L. (2023). Ground penetrating radar forward modeling of roads based on random media model. *Acta Geodaetica et Geophysica*, 58(1), 109-122.

Zhao, W., Tian, G., Forte, E., Pipan, M., Wang, Y., Li, X., Shi, Z., & Liu, H. (2015). Advances in GPR data acquisition and analysis for archaeology. *Geophysical Journal International*, 202(1), 62-71.